

## REDUCTION OF LEAD (II) USING SILVER DOPED ZnO NANOCOMPOSITES

D. F. SHAMS<sup>a</sup>, S. YOUNIS<sup>b</sup>, W. KHAN<sup>b</sup>, I. HUSSAIN<sup>c</sup>, R. ULLAH<sup>d\*</sup>, A. BARI<sup>e</sup>,  
H. M. MAHMOOD<sup>f</sup>, A. NADHMAN<sup>g</sup>

<sup>a</sup>*Department of Environmental Sciences, Abdul Wali Khan University, Mardan, Pakistan*

<sup>b</sup>*Department of Chemistry, Abdul Wali Khan University, Mardan, Pakistan*

<sup>c</sup>*Department of Chemistry, Islamia College University, Peshawar, Pakistan*

<sup>d</sup>*Department of Pharmacognosy (Medicinal Aromatic and poisonous Plants Research Center), College of Pharmacy, King Saud University Riyadh, Saudi Arabia*

<sup>e</sup>*Research Centre, College of Pharmacy, King Saud University, Riyadh, Saudi Arabia*

<sup>f</sup>*Department of Pharmacology College of Pharmacy, King Saud University, Riyadh, Saudi Arabia*

<sup>g</sup>*Institute of Integrative Biosciences, CECOS University, Peshawar, Pakistan.*

Release of lead (Pb) to surface and ground water has been an issue of major concern especially in developing countries with lack of wastewater treatment facilities. Various techniques have been used to remove Pb from domestic and industrial wastewater. In this work, the applicability of silver doped zinc oxide nanocomposite (Ag-ZnO) has been investigated for the reduction of Pb(II) under different experimental conditions. ZnO nanocomposites were modified to doped ZnO by the application of potassium hydroxide (KOH) and subjected to thermal decomposition. The removal was tested at Ag-ZnO dose of 10 µg and 1 µg under the effect of pH (2 to 10) and contact time. The results showed complete reduction of Pb(II) with Ag-ZnO dose of 10 µg as well as 1 µg that corresponded to Ag-ZnO:Pb(II) ratio of 1:200. The treatment was affected by acidic conditions (pH below 3) but effective in the pH range of 4 to 10 with optimum removal at neutral pH. With respect to contact time, 98% of the removal was achieved in the first hour. The findings in this study suggested that Ag-ZnO could be an effective substitute technology to efficiently remove heavy metals from water.

(Received April 8, 2019; Accepted November 4, 2019)

*Keywords:* Doped nanoparticles, Heavy metals, Lead, Zinc oxide, Reduction, Synthesis

### 1. Introduction

Heavy metals (HM) in environment have been a matter of serious concern due to their high toxicity even at low concentrations coupled with their persistence, higher water solubility and mobility, and bioaccumulation in food chain (1). Unlike organic pollutants, heavy metals are non-biodegradable and hence cannot be metabolized and decomposed (2). The United States Environmental Protection Agency has prioritized 13 metals as significant contaminants that include among others, lead, chromium, copper, manganese, mercury, cadmium, nickel, arsenic, zinc, cobalt and antimony (3). Among these, Pb is considered as one of the most significant due to its ubiquitous presence, prolonged persistence and higher degree of toxicity.

---

\* Corresponding author: rullah@ksu.edu.sa

Pb mainly enters into environment from diverse sources such as acid battery manufacturing, metal plating/finishing, paints, plumbing, ammunition and fuel additives among others. Lead poisoning has been linked to severe toxic effects on blood, kidney, nervous system, bones, reproductive system, brain, liver, and thyroid gland with particular risks to children and women (4).

Various techniques have been practiced to remove Pb and other heavy metals from water. These include among others, phytoremediation, adsorption, irradiation, immobilization, membrane filtration, extraction, coagulation, reverse osmosis, ion-exchange and chemical precipitation (5). Each technique offers its own set of advantages however, their application is often limited due to higher operational costs, sophistication in process control and chemical requirement and therefore necessitate the use of more efficient and cutting-edge techniques. Among these, nanotechnology has proved to be highly effective against environmental contaminants (6, 7). This is because of the small size of nanoparticle and the larger surface area per unit mass that allows a greater contact with the surrounding material, and hence increases the reactivity. The high reactivity renders the nanoparticles more efficient and its easy delivery makes them advantageous for *in-situ* application (8).

Recently, metal oxide nanoparticles have been increasingly researched for a variety of applications due to their unique physicochemical properties. Among these, ZnO have received increased attention in the areas of catalysis, optics, magnetism, gas sensing, and piezoelectric (9). ZnO nanoparticles have also been reported to be environmental friendly (10) and therefore, can be used for removal of various contaminants (11) via photocatalysis. However, a major limitation with ZnO nanoparticles is their activation in UV light that reduces its photocatalytic efficacy. Addition of impurities in the form of doping to the nanoparticle lattice has been used to overcome this issue. Doping is the process in which electronic and optical properties of nanoparticles are modified (12). Doping of ZnO can be achieved when  $Zn^{+2}$  atoms are replaced with atoms of higher valence elements. ZnO has been doped by many elements and among these, silver (Ag) doping has shown promise in various applications (13). In this study, ZnO nanoparticle were doped with Ag to modify its optical properties thus increasing its photocatalytic activity by activation in visible range of the electromagnetic spectrum. The study is first of its kind in using doped nanoparticles for the reduction of lead. The purpose was to investigate the photocatalytically enhanced Ag-ZnO nanoparticles for the reduction of the toxic Pb(II) from aqueous solution in visible spectra to inert form thus making it non-toxic. The study was also focused on the effect of pH on the reduction process and the optimum dose of nanoparticle and contact time to complete the reduction process.

## 2. Experimental

### 2.1. Chemicals and reagents

All the chemicals used were of analytical grade and were used without further purification. Silver nitrate ( $AgNO_3$ ); taken as precursor for silver, zinc nitrate ( $Zn(NO_3)_2$ ); taken as precursor for zinc oxide, lead nitrate ( $Pb(NO_3)_2$ ) to prepare synthetic Pb(II) solution and potassium hydroxide (KOH) used as precipitating agent were all purchased from Scharlau, Spain while deionized water (Milli-Q, Millipore) was used for aqueous mediums.

### 2.2. ZnO nanocomposites synthesis

Modified co-precipitation was adopted to synthesize Ag-ZnO nanocomposites (14). Zinc nitrate ( $Zn(NO_3)_2$ ), silver nitrate ( $AgNO_3$ ) and potassium hydroxide (KOH) were used as precursors. Initially, 90 mM of  $Zn(NO_3)_2$  solution was prepared and mixed with 10 mM  $AgNO_3$  solution (10 % doping) in a beaker. Afterwards, 300 mM of KOH solution was added drop wise to the prepared solution with constant stirring. This reaction was carried out at 65 ° C for 2 hours. Afterwards, the nanocomposites were washed three times each with water and ethanol to remove the salts and alkali impurities. The light brown precipitates of nanocomposites were dried in oven at 90° C for 6 hours and were further annealed at 400° C for 3 hours.

### 2.3. Characterization of Nanostructures

The physical characterization of nanostructures was carried out by Transmission Electron Microscopy (TEM), X-ray Diffraction (XRD) analysis, Rutherford Backscattering (RBS) analysis and diffuse reflectance spectroscopy (DRS). The crystallite sizes were confirmed through TEM analysis on a JEOL JEM-1010 transmission electron microscope. The crystallite nature of Ag-ZnO including phases, crystallite structure and crystalline size was measured on a Shimadzu 6000 XRD machine. Analysis was performed using Cu-K $\alpha$  radiation of  $\lambda = 1.54\text{\AA}$ , at 40kV and operating current was set at 30mA. RBS was used for the structure and composition of the synthesized nanocomposites. The detector resolution for RBS was between 15 and 20 keV and the multichannel analyzer was set with a channel width at 5keV. Perkin Elmer UV/VIS/NIR spectrometer-lambda 950 (DRS), with integrating sphere ranges between 900nm to 2500nm was used to check the optical properties of prepared samples.

### 2.4. Experimental setup for treatment of Pb(II) with Ag-ZnO

Synthetic solution of Pb was prepared from analytical grade lead nitrate ( $\text{PbNO}_3$ )<sub>2</sub>. Stock solution of 1000 mg/L was prepared and then diluted to obtain various concentrations of 40 mg/L, 20 mg/L, 15 mg/L, 10 mg/L and 5 mg/L respectively. To find the efficacy of nanocomposites for reduction of Pb(II), Ag-ZnO amounts of 10  $\mu\text{g}$  and 1  $\mu\text{g}$  were tested in visible light using tungsten light (12 lm/W). The Ag-ZnO were used as suspension that was prepared by mixing the nanoparticles in deionized water and then sonicating for 30 minutes. Experiments were first conducted using Ag-ZnO dose of 10  $\mu\text{g}$  and synthetic Pb(II) solutions of 20 mg/L and 40 mg/L that corresponded to a Ag-ZnO:Pb(II) ratio of 1:10 and 1:20 respectively. For each target Pb(II) concentrations, nine batch reactors were setup with different pH conditions ranging from 2 to 10. In the second run, Ag-ZnO dose of 1  $\mu\text{g}$  was used while keeping the same pH conditions in the reactors and Pb(II) concentrations of 20 mg/L and 40 mg/L corresponding to Ag-ZnO and lead ratios of 1:100 and 1:200. Samples were collected after 24 h of the nanocomposites addition. In the third run, contact time was reduced by taking the samples after 6 h and using Pb(II) concentrations of 5, 10, 15 and 20 mg/L and nanoparticle dose of 10  $\mu\text{g}$ . In the final run, the effect of contact time was further assessed with Pb(II) solution of 20 mg/L and NP dose of 10  $\mu\text{g}$  using a sampling interval of 1 h.

### 2.5. Analytical methods

Analysis of Pb was performed using atomic absorption spectroscopy (Hitachi-Z-2000). Data analysis was performed using OriginPro 2018 (Origin-Lab) software.

## 3. Results and discussion

### 3.1. Characterization of synthesized nanostructures

The observed diffraction peaks of the XRD agreed well for the wurtzite hexagonal structure of ZnO. Initially, a few irregular peaks were observed, showing the presence of impurities. After thorough washing, no characteristics peaks of other impurities were observed, which showed the high quality and phase-pure Ag-ZnO nanocomposite (Figure 1) with hexagonal spheroids nanocomposites (Figure 2). The main diffraction peaks were indexed to wurtzite ZnO (hexagonal) appeared at  $2\theta = 31.5^\circ, 34.3^\circ, 36.4^\circ, 47.5^\circ, 56.5^\circ, 62.8^\circ, 66.4^\circ, 68.2^\circ$  and  $69.1^\circ$ . It can be elucidated that a decrease in the peak intensity was noted with in Ag-ZnO. Silver resulted in additional peaks at  $27.2^\circ$  and  $38.1^\circ$  corresponding to Ag related secondary or impurity phase. It is inferred that Ag was both incorporated into the Zn lattice as well as on interstitial sites that occupied substitution site in the ZnO lattice. The sharp peaks further showed that the addition of Ag ions have occupied the zinc lattice without changing the crystal structure, strongly supporting the argument that orientation behavior of ZnO was promoted by Ag doping (13).

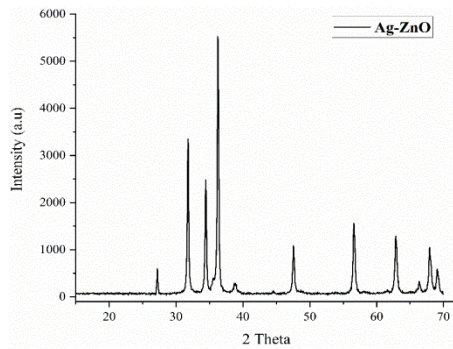


Fig. 1. XRD of the synthesized Ag-ZnO nanocomposites.

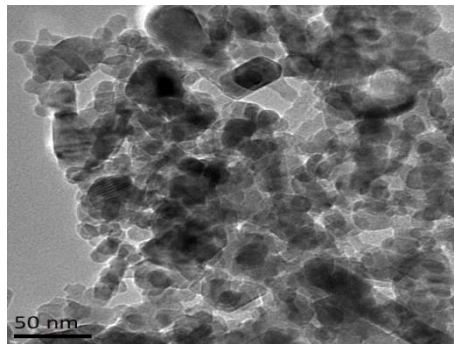


Fig. 2. TEM image of the synthesized nanocomposites, with an average of 22 nm.

Rutherford backscattering (RBS) of Ag-ZnO nanocomposites showed the thickness, defect densities, and structures in the near surface region (Fig. 3). Further, the spectra represented the purity of the nanocomposites.

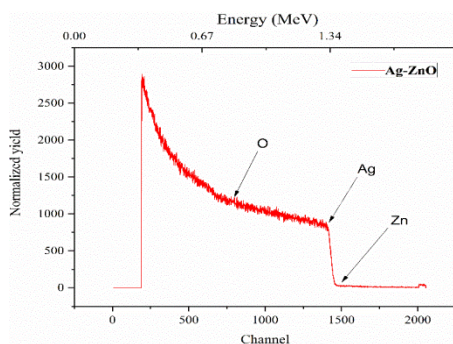


Fig. 3. RBS of the synthesized nanocomposites.

The DRS spectrum of the nanocomposites showed characteristic absorption edges near 450-470 nm representing visible region of the spectrum that are related to the oxygen defects in the nanocomposite structure (Fig. 4). Also, the optical band gap energy was calculated using Kubelka-Munk function;

$$F(R) = [F(R_{\infty}) hv]^{1/2} \quad (1)$$

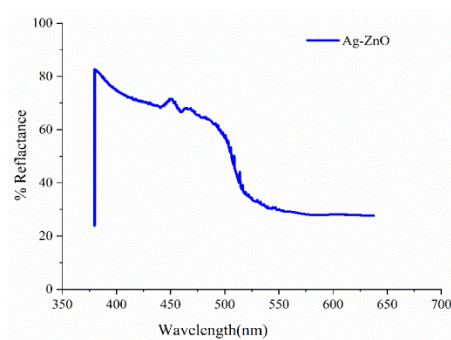


Fig. 4. DRS of the synthesized Ag-ZnO nanocomposites.

where;  $F(R)$  is the Kubelka-Munk function,  $h\nu$  is the energy and  $R$  is the absolute value of reflectance. The energy was derived by plotting the square root of the Kubelka-Munk function  $F(R)^{1/2}$  vs energy in electron volts (eV). Further, band gap energy was estimated from the intercept of tangent drawn to the plot. The band gap of ZnO was shifted to 2.4-2.6 eV from 3.0 eV by doping with Ag, which resulted a change in optical properties of the nanocomposite (Figure 5). This can attribute to the decrease in the band gap energy with the addition of Ag leading to the structural interruption of the ZnO by Ag atoms, which resulted in smaller energy gap between the valence band and conduction band (15).

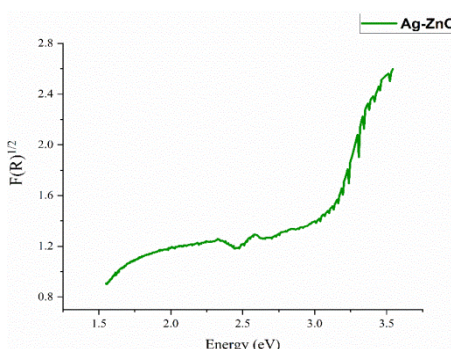


Fig. 5. Bandgap analysis of the synthesized Ag-ZnO nanocomposites.

### 3.2. Reduction of lead (II) and effect of pH

Initially, reduction of Pb (II) was tested with Ag-ZnO dose of 10  $\mu\text{g}$  in Pb(II) solutions of 20 mg/L and 40 mg/L. As shown in Fig. 6, 100% removal was achieved at neutral and alkaline pH with both concentrations. The removal of Pb(II) was comparatively lower in acidic conditions particularly at pH 2 with both the tested Pb concentrations. However, with 40 mg/L at pH 2, the reduction was the lowest at 81%. Though the effect was not pronounced as the efficiency was still more than 80%, the inferior performance indicated that acidic conditions has an inhibitory effect on the Pb(II) reduction with Ag-ZnO. Meanwhile, Ag-ZnO dose of 10  $\mu\text{g}$  proved ample for the tested concentrations. Therefore, in the next phase, Ag-ZnO dose of 1  $\mu\text{g}$  was used in the same Pb(II) solutions and pH range to investigate the efficiency at lower nanoparticle dose. The results showed similar trends in acidic medium, however performance was considerably lower at pH 2 and pH 3 compared to that with 10  $\mu\text{g}$ . At pH 2, 56% removal was observed (Figure 6). Moreover, the trends further confirmed that lower pH affect the reduction of Pb(II) with Ag-ZnO. Whereas, at neutral and alkaline pH, the reduction was maximum as found with 10  $\mu\text{g}$ .

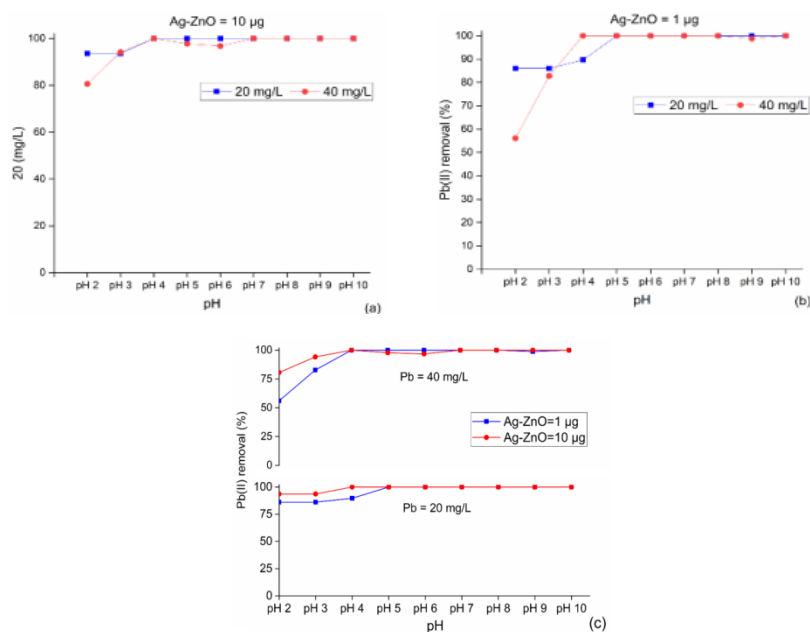


Fig. 6. Reduction of Pb(II) with Ag-ZnO at various pH (a) NP dose of 10 µg (b) NP dose of 1 µg (c) comparison of Pb(II) reduction at 10 µg and 1 µg.

The reduction of Pb(II) with addition of nanoparticles indicated that lead ions interacted with Ag-ZnO nanoparticles and its electronic structure was modified by doping material (16). This can be explained by band theory, which states that; when high energy photon hits a nanoparticle, the electron of its atoms excites and move from lowermost filled valence band to uppermost empty conduction band and is responsible for conductivity while the electron leave holes in the valence band, which behave as positive charge carriers and also moves through the valence band. The concentration of charge carriers in semiconductors is  $10^{21} \text{ m}^{-3}$ , there is space between valence band and conduction band which cannot be occupied by electrons, this space is called band gap or forbidden energy level. Electron in an atom can occupy certain discrete energy states which are called permissible energy level. In ZnO, the bandgap is 3.3 eV, which makes transition more feasible (17), this transition occurred due to doping of material and hence results in reduction of lead. Currently, the Ag doping reduced the bandgap to 2.4 eV thus making it more prone to visible light of the electromagnetic spectrum (Fig. 5). This further helped in enhancing the photocatalytic activity of the nanocomposite, which helped in more generation of reactive oxygen species (ROS) (18).

From Fig. 6, it can be deduced that Pb was reduced by the action of nanocomposite that induced the Pb(II) to gain two electrons thereby converting to non-toxic Pb that has two valence electrons. This mechanism may be explained by the action of ROS, which are generated from the surface of nanocomposites when exposed to light (19). Afterwards, Ag-doped ZnO nanocomposites interacted with Pb(II) in the presence of visible light (12 lm/W) while the unpaired electrons from ROS reacted with Pb(II) and reduced it to its lower oxidation state i.e. from  $\text{Pb}^{2+}$  to  $\text{Pb}^{1+}$  and further reaction reduces  $\text{Pb}^{1+}$  to a non-charged  $\text{Pb}^0$ .

### 3.3. Effect of contact time on Pb(II) reduction

To determine the reduction of Pb(II) with Ag-ZnO as a function of time, the time to take the sample was reduced to 6 h from 24 h. A nanoparticle dose of 10 µg and Pb(II) concentrations of 5, 10, 15 and 20 mg/L were used while the pH was kept as neutral (pH 7). A removal of 100% was observed after 6 h with all the tested concentrations. Therefore, in the next step, using a single Pb(II) concentration of 20 mg/L, the sampling time was further reduced to 1 h. As evident from Figure 7, 98% of the Pb was reduced within the first hour of the contact and nearly 99% was removed after 2 h. In the first hour maximum removal was achieved and as the contact time between lead and

nanocomposite increased in the subsequent 4 hours, Pb(II) reduction was completed. The observed rate of reduction in this study was higher compared to other nanoparticles used for heavy metals such as 21 hours by Boparai et al., (20) for the removal of Cd (II) via adsorption with zero-valent iron nanoparticles with initial concentration of 112 mg/L. Meanwhile, from the observed trend for the period of 4 hours, the reaction rate could not be truly inferred since 98% of the activity happened in the first hour and the reduction reached towards almost an equilibrium in this time. Further investigation would be required to further reduce the reaction time to correctly establish the reduction rates with Ag-ZnO.

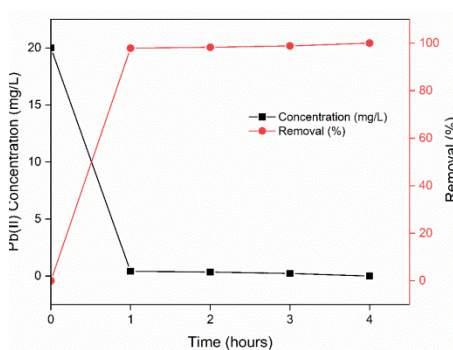


Fig. 7. Effect of contact time on Pb(II) reduction with Ag-ZnO.

#### 4. Conclusions

The application of Ag doped ZnO nanocomposite proved as a highly efficient technique for the removal of Pb(II) via reduction. The Ag-ZnO nanocomposite dose from 10  $\mu\text{g}$  to as low as 1  $\mu\text{g}$  completely removed Pb(II) from water at Ag-ZnO:Pb(II) ratio of 1:200. The treatment was effective in the pH range of 4 to 10. A pH value of less than 3 in the medium retarded the reduction while neutral pH conditions were optimum. The contact time required for the treatment was less as 98% of the removal was achieved in the first hour. Further modifications could be made such as decreasing the contact time to less than an hour to truly ascertain the kinetic rates and performing the study with real effluent to establish the efficacy of Ag-ZnO nanocomposite in field applications. Further, we are also focusing on the use of higher intensity LEDs or sunlight (which contain more visible portion of the electromagnetic radiation) to assess the efficacy of such nanocomposites.

#### Data Availability

The data used to support the findings of this study are available from the corresponding author upon request.

#### Conflicts of Interest

The authors declare no conflict of interest.

#### Acknowledgments

The authors extend their appreciation to the Research Supporting Project No (RSP-2019/110) King Saud University Riyadh Saudi Arabia for financial support.

## References

- [1] S. Rajput, L. P. Singh, C. U. Pittman, D. Mohan, *Journal of Colloid and Interface Science*. **492**, 176 (2017).
- [2] Ge F, Li M-M, Ye H, Zhao B-X., *Journal of Hazardous Materials*. **211**, 366 (2012).
- [3] Yu B, Zhang Y, Shukla A, Shukla SS, Dorris KL., *Journal of Hazardous Materials*. **80**(1), 33 (2000).
- [4] Flora SJS, Agrawal S. Chapter 31 - Arsenic, Cadmium, and Lead. In: Gupta RC, editor. *Reproductive and Developmental Toxicology (Second Edition)*: Academic Press; 2017. p. 537-66.
- [5] Liu Y, Lou Z, Sun Y, Zhou X, Baig SA, Xu X., *Microporous and Mesoporous Materials*. **246**, 1 (2017).
- [6] Anjum M, Miandad R, Waqas M, Gehany F, Barakat M., *Arabian Journal of Chemistry*. (2016).
- [7] Wang X, Guo Y, Yang L, Han M, Zhao J, Cheng X., *Journal of Environmental and Analytical Toxicology*. **2**(7), 1000154 (2012).
- [8] Tafazoli M, Hojjati SM, Biparva P, Kooch Y, Lamersdorf N., *Journal of Plant Nutrition and Soil Science*. **180**(6), 683 (2017).
- [9] Verma SK, Panda PK, Jha E, Suar M, Parashar S., *Scientific Reports*. **7**(1), 13909 (2017).
- [10] Khezamia L, Tahaa KK, Amamic E, Ghiloufid I, El Mird L., *Desalination and Water Treatment*. **62**, 346 (2017).
- [11] Rizwan M, Singh M, Mitra CK, Morve RK., *Journal of Nanoparticles*. **2014** (2014).
- [12] Kwon SG, Chattopadhyay S, Koo B, dos Santos Claro PC, Shibata T, Requejo FIG, et al. *Nano letters*. **16**(6), 3738 (2016).
- [13] Nadhman A, Nazir S, Khan MI, Arooj S, Bakhtiar M, Shahnaz G, et al. *Free Radical Biology and Medicine*. **77**, 230 (2014).
- [14] Arooj S, Nazir S, Nadhman A, Ahmad N, Muhammad B, Ahmad I, et al. *Beilstein Journal of Nanotechnology*. **6**(1), 570 (2015).
- [15] Kim Y-S, Park C., *Physical Review Letters*. **102**(8), 086403 (2009).
- [16] Chen X, Burda C., *Journal of American Chemical Society*. **130**(15), 5018 (2008).
- [17] Naveed Ul Haq A, Nadhman A, Ullah I, Mustafa G, Yasinzai M, Khan I., *Journal of Nanomaterials*. **2017**, 14 (2017).
- [18] Nadhman A, Khan MI, Nazir S, Khan M, Shahnaz G, Raza A, et al., *International Journal of Nanomedicine*. **11**, 2451 (2016).
- [19] Abdal Dayem A, Hossain MK, Lee SB, Kim K, Saha SK, Yang G-M, et al. *International Journal of Molecular Sciences*. **18**(1), 120 (2017).
- [20] Boparai HK, Joseph M, O'Carroll DM., *Journal of Hazardous Materials*. **186**(1), 458 (2011).